

Adulterated beef detection with redundant gas sensor using optimized convolutional neural network

Ardani Cesario Zuhri¹, Agus Widodo¹, Mario Ardhany¹, Danny Mokhammad Gandana¹, Galang Ilman Islami¹, Galuh Prihantoro²

¹Research Center for Process and Manufacturing Industry Technology, Research Organization for Energy and Manufacture, National Research and Innovation Agency, Jakarta, Indonesia

²Research Center for Electronics, Research Organization for Electronics and Informatics, National Research and Innovation Agency, Jakarta, Indonesia

Article Info

Article history:

Received Jul 18, 2024

Revised Feb 11, 2025

Accepted Mar 11, 2025

Keywords:

Adulterated beef
Convolutional neural network
Machine learning
Pork adulteration
Redundant gas sensor

ABSTRACT

Various types of research have been developed to detect beef adulteration, but the accuracy and reliability of these results still require improvement. This study proposes designing a highly precise redundant electronic nose system using an optimized convolutional neural network (CNN) method to detect adulterated beef mixed with pork. As baselines, other classifiers are also utilized, namely the decision tree (DT), K-nearest neighbor (KNN), artificial neural network (ANN), and support vector machine (SVM). Several data preprocessing methods are employed to increase prediction accuracy, namely feature selection, principal component analysis (PCA), and time series smoothing. The weight of each data sample was 100 g with 15 classes of pork and beef mixing ratios of 0%, 0.1%, 0.5%, 1%, 5%, 10%, 20%, 30%, 40%, 50%, 60%, 70%, 80%, 90%, and 100% pork. With the single-layer sensor configuration, the average CNN classification success rates were 97.15%, 96.29%, and 99.64% for layers 1, 2, and 3, respectively. In addition, from the combination of the three layers, a prediction results of 99.72% was obtained. Thus, a redundant gas sensor array configuration can improve the classification results. In addition, the relatively high accuracy of the optimized CNN provides a convincing alternative for identifying possible beef adulteration.

This is an open access article under the [CC BY-SA](#) license.



Corresponding Author:

Ardani Cesario Zuhri

Research Center for Process and Manufacturing Industry Technology

Research Organization for Energy and Manufacture, National Research and Innovation Agency

Jakarta, Indonesia

Email: arda004@brin.go.id

1. INTRODUCTION

Beef is a high-quality food that contains nutrients, niacin, vitamin B, iron, and a complete source of protein that can improve health, growth, muscle building, cells, and hormones in the human body [1]. However, adulterated beef (with pork) is still commonly found in the markets, such as in Indonesia and Korea [2], [3]. The practice of adulteration involves mixing and blending meat from different species to obtain excessive profits at a lower cost [4]. The impact of this meat fraud is very harmful to consumers, especially Muslims who prioritize halal food, and it seriously restricts the progress of local meat businesses [5]. Therefore, an instrument specifically designed to detect beef adulteration is urgently needed.

Several scientific instruments and methods for detecting beef adulteration have been developed, including gas chromatography (GC) and mass spectrometry (MS) [6], hyperspectral imaging (HSI) [7],

polymerase chain reaction (PCR) technology [8], and fourier transform infrared (FT-IR) spectroscopy [9]. However, some research instruments and methods require further consideration, such as specific laboratory capabilities, test samples damaged by destructive testing, expensive costs, and extended test times [10]. Therefore, a scientific instrument and method that can detect beef adulteration quickly, cheaply, precisely, and reliably is needed using an electronic nose (e-nose). The application of e-nose with aroma recognition has been tested in the automotive field to detect the concentration level of vehicle exhaust gas [11], in the health sector to detect bacterial infections [12], and in the food sector to detect meat freshness [13]. The application of e-nose has also successfully detected adulteration in lamb and duck meat using a combination of backpropagation neural network (BPNN) and support vector machine (SVM), obtaining an accuracy of 98.59% [14]. In the preceding study, the E-nose successfully detects pork adulteration by integrating gas and colorimetric sensors with the result of 91.27% accuracy in training and 87.5% in prediction [15]. The e-nose application successfully detected pork adulteration with beef for halal authentication using nine different sensors and seven classes of meat mixture proportions. In addition, it used an optimized SVM recognition model with an accuracy of 98.1% [16].

One of the main components of the e-nose is the use of multiple gas sensors. However, the gas sensor suite has several disadvantages compared with other sensors, including low sensitivity to low gas concentrations, poor selectivity, sensor aging, leading to errors, and data corruption [17]. Several options to mitigate the drawbacks of sensor replacements have been proposed, including fault correction [18], fault detection [19], or classification algorithmic [20]. Another alternative to prevent damage or failure of sensor readings is to use redundant information from the sensor array [21], [22]. By using redundant information from multiple sensors, the e-nose system can reduce the risk of single sensor errors and provide greater certainty to the decisions made, thus improving the ability to identify and detect beef adulteration.

In beef adulteration detection, several researches have also shown that machine learning, particularly the convolutional neural network (CNN) architecture, has an excellent potential to improve model accuracy. The CNN algorithm can reduce noise in extensive datasets through image and spectral data, where new features are generated with lower entropy after convolution [23]. CNNs have been widely used in image recognition using 2D convolution [24]-[27], and have also been successfully applied to time series domains using 1D convolution [28]-[31]. CNN was also successfully applied to identify milk powder counterfeiting with an average accuracy of 97.8% [32] and honey counterfeiting with an average accuracy of 100% for a model with 32 kernels and a 7×1 filter size [33].

This study proposes an e-nose design with redundant gas sensors to detect beef and pork adulteration using an optimized CNN algorithm. In this study, the decision tree (DT), K-nearest neighbor (KNN), artificial neural network (ANN), and SVM methods were also used to compare the accuracy results of several other classifications. The research questions addressed by this study consists of the following: i) is the use of redundant layers of a gas sensor array capable of improving classification accuracy?; ii) is a one-dimensional (1D) CNN suitable for categorizing a dataset of gas emissions from mixed beef and pork; and iii) what are the most influential sensor types for identifying adulterated beef?. Furthermore, the primary contributions of our proposed approach comprise of: i) constructing redundant layers of the gas sensor array, where each layer consists of 8 gas sensor; ii) demonstrating the suitability of an optimized CNN for categorizing a dataset of gas emissions from mixed beef and pork; iii) identifying the most influential sensor types for identifying adulterated beef. Combining the e-nose design and the developed classification model will result in a cheap, practical, and precise system for detecting beef adulterated with pork.

2. METHOD

2.1. Material sample preparation and electronic nose design

The research objects in this test were pork and beef. Both types of meat were obtained from the Butchery section at Serpong, South Tangerang, Indonesia. The meat was stored in a freezer at 17 °C prior to testing. The meat samples (Figures 1(a) and (b)) weighed 100 g with 15 classes of pork and beef mixing ratios, consisting of 0% (0:100), 0.1% (0.1:99.9), 0.5% (0.5:99.5), 1% (1:99), 5% (5:95), 10% (10:90), 20% (20:80), 30% (30:70), 40% (40:60), 50% (50:50), 60% (60:40), 70% (70:30), 80% (80:20), 90% (90:10), and 100% (100:0). The mixing ratio was set to the least possible mixing ratio of 0.1 g pork to ensure that the system could detect relatively little pork in the beef.

The meat samples were placed in a redundant gas sensor array chamber. Gases generated by the samples produce odors that are detected by gas sensors. The resistance levels of gas sensors change depending on the amount of gases detected. Resistance values of gas sensors are converted into voltage data and then sent to Raspberry Pi 4B using analog-to-digital converter (ADC) modules. The Raspberry data will be processed utilizing Python programming language. Figure 1(c) shows the design of the sensor chamber, which has a length, width, and height of 350, 250, and 250 mm, respectively.

The gas sensor is a semiconductor manufactured by Winsen Electronics. The redundant gas sensors comprise eight different gas sensors with three replicas and one temperature and humidity sensor, as shown in Table 1. Redundant gas sensors ensure that adulteration detection systems can function correctly and precisely even if some sensors are less sensitive or damaged and can improve classification accuracy by removing noncontributing or irrelevant features [34], [35]. There are three layers, each with eight different gas sensors. The topmost layer in the chamber box is layer 1, followed by layer 2 below it, and layer 3 at the bottom of the arrangement. Each layer was designed with a distinct diameter to optimize odor emission from beef, ensuring detection by all sensors inside each layer. The diameters of the first, second, and third layers were 50, 95, and 140 mm, respectively. The spacing between each layer was 30 mm, and the distance between the meat and closest layer 3 was 150 mm.

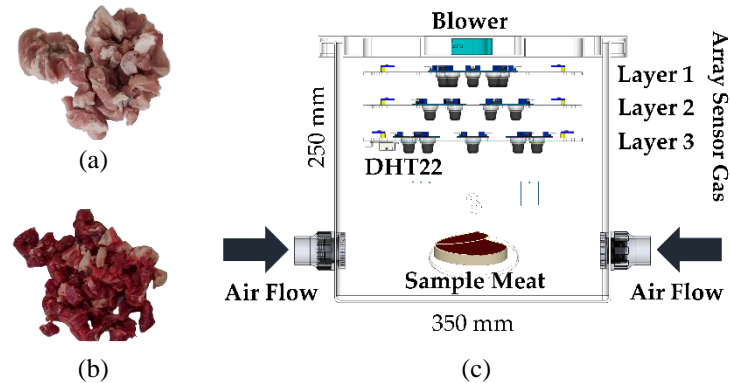


Figure 1. Preparation of test samples; (a) pork, (b) beef, and (c) design of the sensor chamber

Table 1. Redundant gas sensor arrays

Layer 1		Layer 2		Layer 3		Sensor description
No	Initial sensor	No	Initial sensor	No	Initial sensor	
1	MQ2_1	9	MQ2_2	17	MQ2_3	MQ2 detects smoke, hydrogen, LPG, alcohol, and methane
2	MQ4_1	10	MQ4_2	18	MQ4_3	MQ4 detects natural gas and methane (CH ₄)
3	MQ6_1	11	MQ6_2	19	MQ6_3	MQ6 detects iso-butane, propane, and LPG
4	MQ9_1	12	MQ9_2	20	MQ9_3	MQ9 detects CO, propane, and methane
5	MQ135_1	13	MQ135_2	21	MQ135_3	MQ135 detects CO ₂ , benzene, NH ₃ , NO _x , and alcohol
6	MQ136_1	14	MQ136_2	22	MQ136_3	MQ136 detects H ₂ S, hydrogen, CO, and methane
7	MQ137_1	15	MQ137_2	23	MQ137_3	MQ137 detects ammonia, hydrogen, and ethanol
8	MQ138_1	16	MQ138_2	24	MQ138_3	MQ138 detects aromatic and other organic solvents

The gas sensor was first turned on to warm up for 120 min, and the chamber cover was then opened for cleaning to obtain clean air. For sample preparation, meats were moved out from the freezer and left at room temperature for 120 min. The test parameters were as follows: initial data collection for clean air for 60 min; data collection for each class of samples for 60 min; sampling interval for 1 s; and gas and air cleaning time for 2 min. The first and second configurations use single-sensor layer data points and three-sensor layer data points, respectively. Each 10 data points was averaged together to reduce variability and the effect of outliers or extreme values. The first configuration with eight gas sensors on a single layer has 8 sensors×60 min×6 points/minutes×15 classes=43,200 data points. The second configuration with three layers has 43,200×3 layers=129,600 data points. Thus, the number of samples was 43,200 data points/8 sensors or 129,600 data points/24 sensors, which is equal to 5,400 records.

2.2. Feature selection

Feature selection is a dimension reduction technique that reduces feature complexity by selecting a subset of the original features that are distinguishable from each existing classes [36]. These relevant features lead to good learning in terms of accuracy, computational cost, and model interpretability. In this study, feature selection combined the filter and wrapper methods. In the filter method, the preprocessing step is not influenced by the choice of a predictor. The F-test, mutual information (MI), and Pearson's correlation coefficient (PCC) are utilized for filtration methods. The F-test examines the value of variance between groups compared with that within groups [37]. The information gain (IG) is computed through the MI between features X_i and class Y to examine the dependency between features and labels [28]. Meanwhile, the Pearson correlation coefficient determines the linear correlation between two variables by computing the

ratio between their covariances and the product of their standard deviations [38]. The wrapper method determines the most influential features using the prediction results from the classifier. The proposed model is relatively reliable because of its ensemble capability in combining prediction results from several data subsets [39]. Next, selected features are ordered by their relevance according to the number of rankings from each selected feature selection method, which is usually called the Borda count [40].

2.3. Principal component analysis

In addition to feature selection, feature extraction is another dimensional reduction method that combines the fractions of features into other sets of features or principal components in principal component analysis (PCA) [41]. PCA projects features into multiple dimensions via orthogonal transformations that preserve maximum variance [42]. In addition, this method is renowned for data reduction without forfeiting prominent information [43]. The PCA group data covariance was determined by ranking the eigenvalues from highest to lowest. The covariance value of the data matrix with the highest eigenvalue aligns all data with the highest approximation [44].

2.4. Convolutional neural network for time-series prediction

The data produced by the sensor are in the form of a time series with a specific fluctuating pattern. Therefore, this study employs classification techniques to capture time series patterns. Recent studies have indicated that CNN, especially 1D CNNs, have yielded outstanding results for time series domains [28]-[31]. The architecture of the 1D CNN for time series data from sensor readings is shown in Figure 2. It consists of an input layer, two 1D convolutional layers, one max pooling layer, one flattening layer, one completely connected hidden layer, and a multiclass output layer. The input data of the CNN have a 3D form consisting of several samples, time steps, and features. The features consist of eight sensors for each layer in the three-layer arrangement. The proposed CNN model employs 1D convolution kernels that stride the time series to extract temporal features. Out of these features, their values of a specific size are pooled to obtain a summary of each group, such as the maximum value for each group. The proposed pooling reduces the number of features and noise. Finally, the pooled results are flattened into a 1D array before being fed into the dense neural network layer.

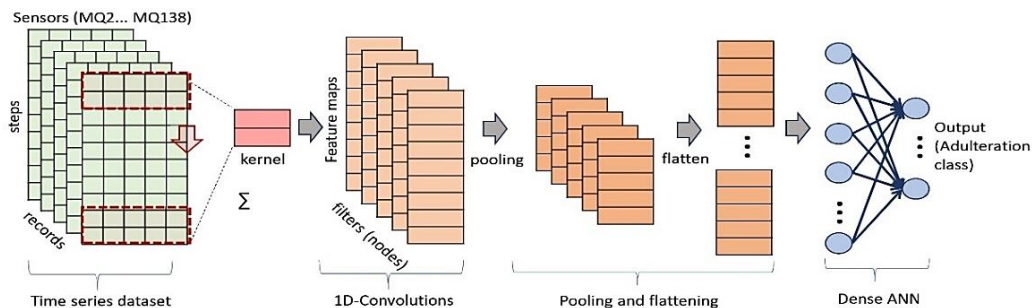


Figure 2. A 1D CNN classification framework based on olfactory sensor data

This study proposes an optimum length of time steps that determines the output of a time series. The importance of specifying the time step size in a time series was previously described in [45], [46]. The experimentation of various lengths of time steps is made possible by CNN because it requires at least 2D input shapes for each sample, hence 3D shapes in total. In addition, the number of hidden nodes in the convolutional layers is optimized via a grid search of possible combinations of hidden node numbers. The experiment was implemented using Python code, as described in [47], and ran in the Google Colaboratory environment, which hosts the Jupyter Notebook service.

3. RESULTS AND DISCUSSION

3.1. Gas sensor dataset

The e-nose sensors generate a ratio between the initial resistance and measured resistance (R_s/R_o) data of as many as 5,400 records in 15 classes. Thus, each class comprises 360 samples. Figure 3 shows the different ranges of values for each class of the time series, although there are some overlaps among the data from different sensors. Figure 3(a) indicates that the sensors at the 1st layer, which was placed furthest from the gas source, exhibit more stable patterns, whereas one sensor (MQ9) at the 2nd layer exhibits a fluctuating

pattern Figure 3(b). In addition, most sensors in the third layer, which is placed closest to the gas source Figure 3(c), exhibit fluctuating patterns. Although the sensor patterns in Figure 3 appear to overlap, their differences among classes are better than those of the other two layers.

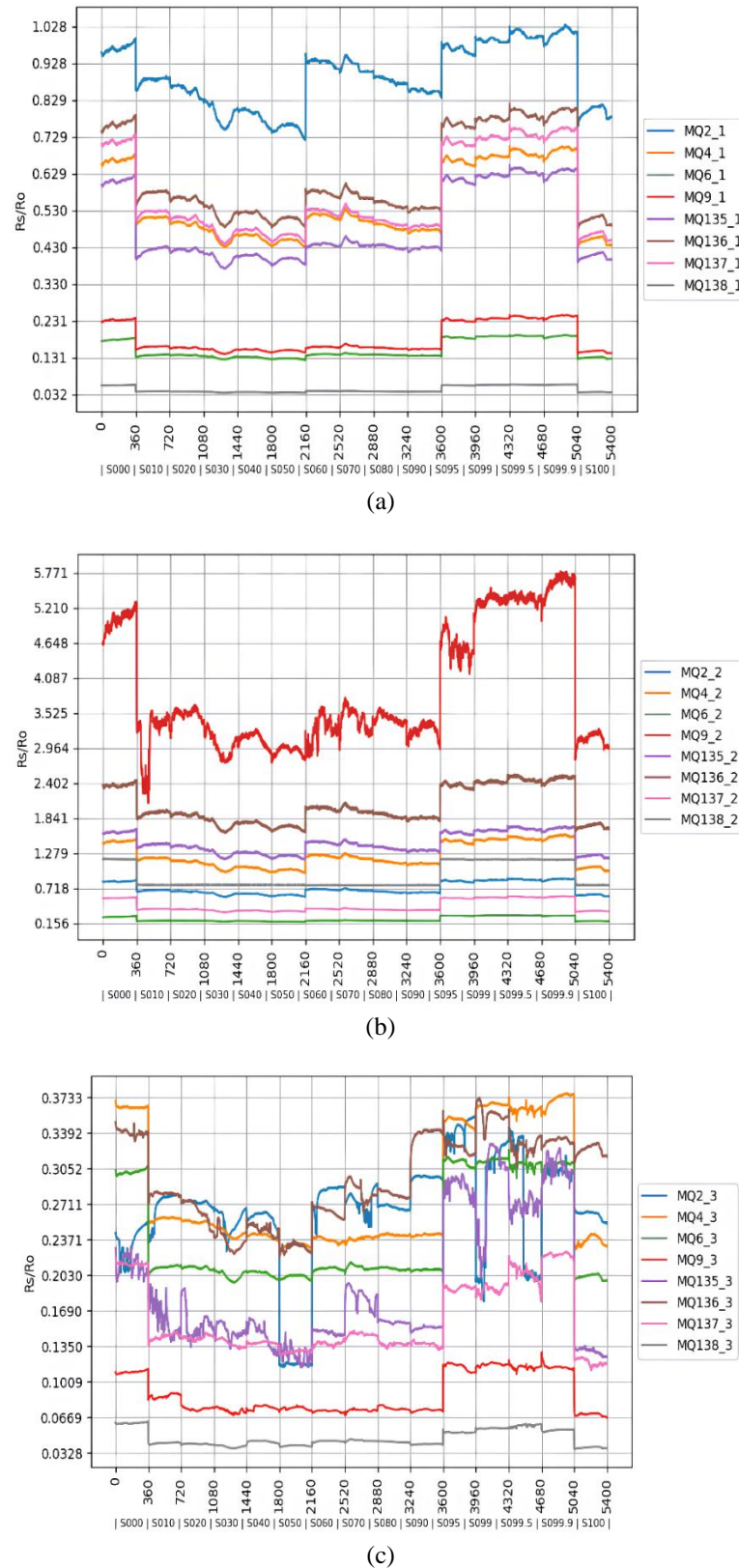


Figure 3. Patterns of time series sensor data for; (a) layer 1, (b) layer 2, and (c) layer 3

3.2. Redundant gas sensor selection

Based on the rank of scores from each feature selection method, the most selected sensors in layer 1, in ascending order, are: {MQ9_1, MQ137_1, MQ2_1, MQ4_1, MQ6_1, MQ135_1, MQ136_1, and MQ138_1}, while the most selected sensors for layer 2 and layer 3 are {MQ138_2, MQ137_2, MQ2_2, MQ4_2, MQ6_2, MQ135_2, MQ9_2, and MQ136_2}, and {MQ138_3, MQ4_3, MQ137_3, MQ136_3, MQ6_3, MQ9_3, MQ2_3, and MQ135_3}. Table 2 lists the ranks of each method at each layer and their total counts. When the three layers are used at once, which means 24 features in total, the top five most selected sensors are MQ138_3, MQ137_3, MQ137_2, MQ137_1, and MQ136_1. By contrast, MQ9_2, MQ136_2, MQ135_3, MQ4_2, and MQ6_2 were the least selected sensors. In addition, among all classifiers, their prediction accuracy tended to increase starting from using 40% of features, or approximately three features for the first, second, and third layers, and approximately ten features for the combination of all layers. Specifically, based on the cross-validation results, the most optimal percentage of selected features was 90% for layers 1 and 2 (or $0.9 \times 8 \approx 7$ features), 80% for layer 3 (or $0.8 \times 8 \approx 6$ features), and 50% for the combination of all layers (or $0.5 \times 24 \approx 12$ features).

Table 2. Ranking of each feature in layers 1, 2, and 3

Methods	MQ2			MQ4			MQ6			MQ9			MQ135			MQ136			MQ137			MQ138		
	1	2	3	1	2	3	1	2	3	1	2	3	1	2	3	1	2	3	1	2	3	1	2	3
F-Score	1	5	1	3	4	7	6	6	8	7	1	4	5	2	2	2	3	3	4	7	5	8	8	6
MI	8	6	6	6	7	5	2	2	2	3	3	1	4	8	3	5	5	7	7	4	4	1	1	8
PCC	1	6	1	5	2	7	3	1	5	6	4	6	2	3	3	8	5	2	7	8	8	4	7	4
RF	8	4	3	4	5	7	7	8	1	6	7	4	5	3	2	1	1	6	2	2	5	3	6	8
Total	18	21	11	18	18	26	18	17	16	22	15	15	16	16	10	16	14	18	20	21	22	16	22	26

3.3. Data dimensional reduction

Features were extracted using PCA for several principal components (PCs). The eigenvalues presented in Table 3 denote that principal component 1 (PC1) alone contributed 97.26% of the variance. The addition of PC1 and PC2 results in more than 99% of the cumulative variance, which is adequate to represent all eight features. The variance threshold for PC retention is about 70-85% to guarantee that PCs can retain most of the information of the original variables [48], [49]. In addition, Figure 4 shows the clustering of data based on the number of PCs. Figure 4(a) shows two PCs in layer 1. All data in the same class are relatively grouped and Figure 4(b) shows three PCs of different classes.

Table 3. Eigenvalues and proportions of variance in PCA at layer 1

Calculation	Components							
	PC1	PC2	PC3	PC4	PC5	PC6	PC7	PC8
Eigenvalue	77.960	0.2052	0.0097	0.0024	0.0009	0.0005	0.0002	0.0002
Proportion of variance	97269%	2560%	0.12%	0.03%	0.01%	0.01%	0.00%	0.00%
Cumulative	97269%	99830%	99951%	99980%	99992%	99997%	99999%	100%

High prediction accuracy of all classifiers can be achieved using a certain number of PCs. The first layer achieved the best accuracy using 90% of its eight features, and the second and third layers achieved the best accuracy using 80% of their eight features. The combination of all layers required 50% of its 24 features to yield the best performance.

3.4. Smoothing

Smoothing is a technique used to reduce variations in time series data or overcome the presence of outliers [50]. In this study, the simple moving average, which averages a predecided number of successive data points with equal weights, is applied to smooth the time series. Several options are provided to obtain the optimal length of the averaged points: odd numbers running from a short to an arbitrarily long number, namely 3 to 45. Odd numbers were chosen to be evenly divided to their median left and right. The classifiers were then run against the smoothed data of those lengths, and the best average classification performance for that length was obtained. The cross-validation results indicate that 37 is the optimal length for the DT, 31 for the KNN and ANN, 25 for the SVM, and 17 for the CNN.

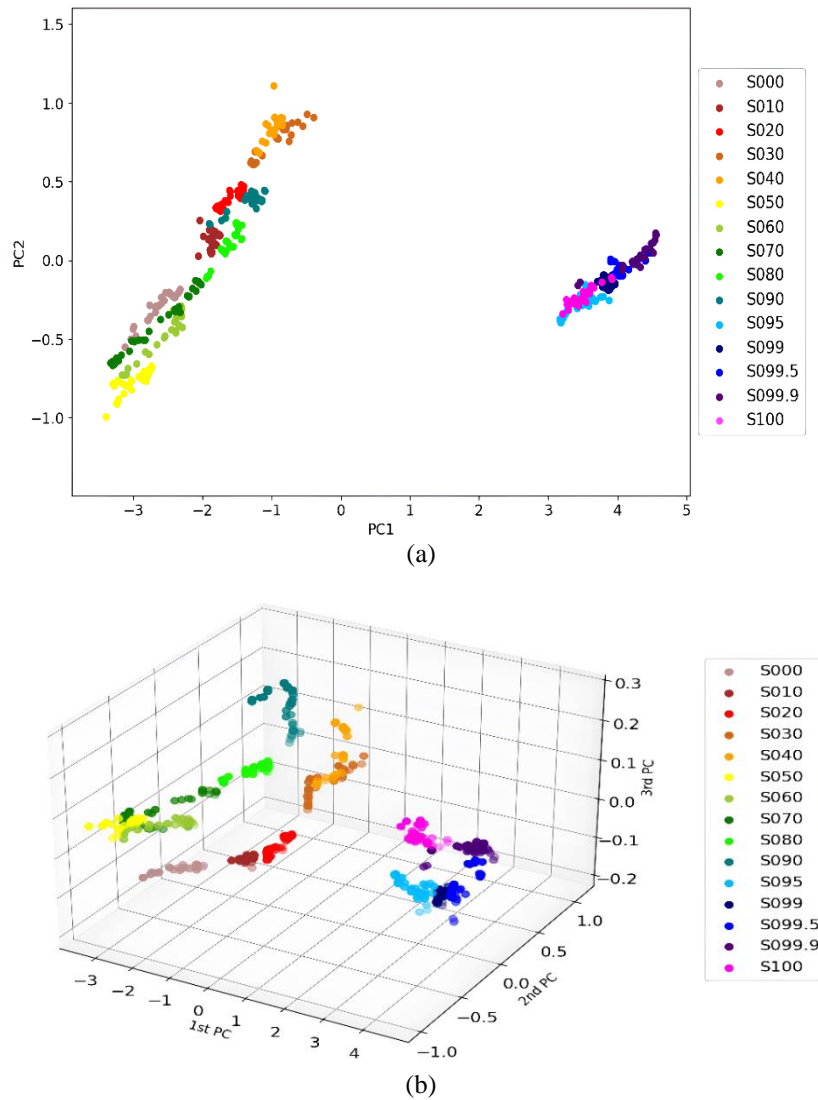


Figure 4. Data grouping based on the number of principal components; (a) data grouping using two PCs and (b) data grouping using three PCs

3.5. Classifier optimization

3.5.1. Convolutional neural network

Several parameters in the CNN must be optimized to obtain the best performance. Here, one of them is the length of the sequence steps of a time series. As shown in Figure 5, the CNN sample was constructed from the original data into 3D data, with each sample consisting of sensors with specific sequence steps. Short steps may not capture the time series pattern; however, long steps may lose a specific pattern. Thus, several length options are provided, and the CNN is run against the time-series data of that length. Among the length options, namely 15 to 330 points with a multiple of 15, the length that best performs the CNN is 150 (Figure 6). Accordingly, from the total 5,400 datasets of 15 classes, the previous 360 data points are now 210 time-series data per class.

In addition, other parameters to optimize include the number of hidden nodes (called filters) in the convolution layer and the number of nodes in the dense layer. Because there are two convolution layers in this experimental setup, both layers are given the same initial number of nodes, starting from 16 to 200 with a multiple of 16. Out of these numbers, cross-validation was employed to obtain the optimal combination of both layers, which yielded the highest classification accuracy. The best performance was obtained by combining 176 and 128 nodes in layers 1 and 2, respectively. Similarly, another cross-validation was performed to obtain the best number of nodes in the dense layer. Given an initial number of 10 to 200, a multiple of 10 and 150 is the best node number for the dense layer (Figure 6).

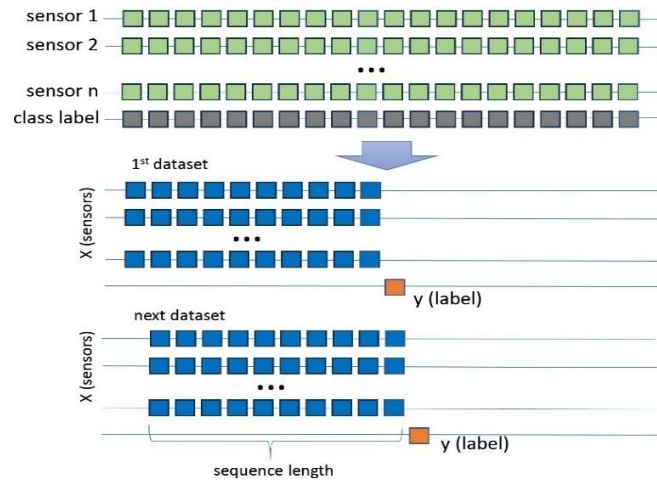


Figure 5. Time series dataset with each sample comprising sensor data of a specific length

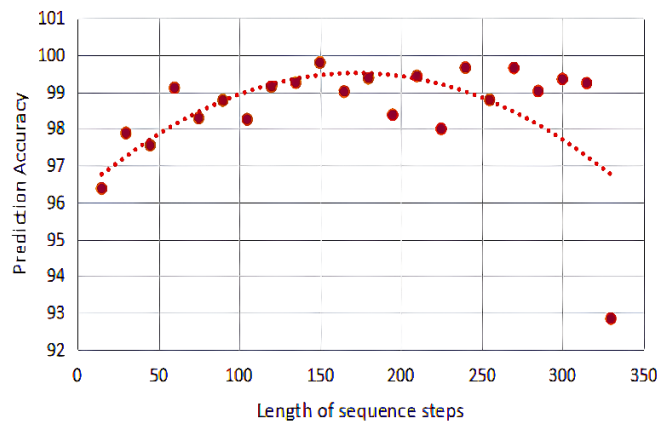


Figure 6. Optimal length of time series sequence

The final parameters of the CNN to be optimized are the kernel size, pooling kernel size, and the percentage of dropout nodes. As stated in [51], smaller kernel sizes are better choices than larger sizes because they better retain the locality of the extracted features. Similarly, [52] indicated that the size of the pooling kernel should always be small to avoid significant information loss in feature quality. During the experiment, cross-validation was used to select the size of the kernel and the maximum pooling kernel for the classifiers applied at layers 1, 2, and 3. The initial sizes were 2, 3, 4, and 5. The best result among these values was obtained using the kernel and maximum pooling with a size of 2.

Similarly, the optimal percentage of dropout nodes was obtained via cross-validation. The dropout technique can prevent overfitting and efficiently approximate a combination of different neural network architectures [53]. For CNNs, [54] indicated that 10% and 20% dropouts are preferable. In this experiment, when the dropouts are applied after the convolutional and dense layers, their initial values are designated as 10%, 20%, 30%, 40%, and 50%. It turns out that 10% is the optimal dropout value.

3.5.2. Baseline classifiers

This study uses simple classifiers to compare the performance of CNNs, namely the DT and KNN, as well as the more sophisticated ones, namely the ANN and SVM. The parameters of these classifiers were also optimized by cross-validation on the training dataset. For the DT, the optimal depth of the tree was determined by providing initial values of 3-20. The depth at which the best performance was achieved was 11. Similarly, the KNN's best number of neighbors is one out of the given numbers from 1 to 10.

The ANN, which uses two hidden layers in this experiment, initially provides several nodes with a range of 16 to 200 with a multiple of 16. The number of nodes suitable for both hidden layers was 128. For

the number of epochs, the optimal values of the ANN and CNN determined by cross-validation were 180 and 220, respectively. The SVM hyperparameters are constant C and gamma, which control the optimal fit of the classification boundary. The C and gamma parameters were selected from several possible combinations, such as {0.1, 1, 5, 10, 50, 100, 500, 1000} and {0.05, 0.1, 0.5, 1, 2}, respectively. The optimal combinations of both values are 500 and 1.

3.6. Classifier performance

The five classifiers employed during the experiment, DT, KNN, ANN, SVM, and CNN, were run against eight features in one of three layers; the average values of the eight features in all layers, the median values of those features, or the total of 24 features in all layers. Table 4 shows the classification accuracy of each classifier using the original features, selected features, extracted features as PCs, and smoothed features. In addition, the percentage of data used for training and testing was 10% and 90%. This relatively small number of training samples was selected to allow easy determination of difference in accuracy. The performance accuracies of predictors with that training number were greater than 85%, and some even reached 100%.

Table 4. Classifier performances for different features and layer configurations

Classifiers	Feature	Layer 1 (%)	Layer 2 (%)	Layer 3 (%)	Layers 1, 2, and 3 (%)
DT	Original features	93.21	92.16	98.75	97.9
	Feature selection	95.25	91.79	98.17	98.46
	PCA	97.9	90.91	98.91	98.85
	Smoothing	96.21	97.1	99.29	99.68
KNN	Original features	98.25	96.67	99.98	99.98
	Feature selection	98	96.81	99.96	99.96
	PCA	97.9	92.1	99.88	100
	Smoothing	99.46	99.24	99.82	99.93
ANN	Original features	91.46	94.03	99.79	99.96
	Feature selection	93.13	94.01	99.36	99.88
	PCA	93.13	94.01	99.36	99.88
	Smoothing	92.19	96.52	100	100
SVM	Original features	99.59	97.84	99.9	99.98
	Feature selection	98.99	97.94	99.94	99.98
	PCA	99.53	97.1	99.9	99.98
	Smoothing	99.58	99.47	100	100
CNN	Original features	99.61	99.54	100	100
	Feature selection	99.75	99.79	100	100
	PCA	100	99.37	99.79	99.89
	Smoothing	99.92	99.5	100	100

CNN outperformed the other classifiers with an accuracy of 99.82%, followed closely by the SVM with an accuracy of 99.36%. As a simple classifier, the KNN also yields excellent results with 98.62% accuracy, which is greater than the performance of the ANN and DT with accuracy values of 96.67% and 96.53%, respectively. Based on this result, we assume that a 1D CNN is suitable for a time-series based sensor dataset.

However, data preprocessing and dimensionality reduction yield mixed results. Smoothing increased the performance of most classifiers with an average accuracy of 98.90%. In contrast, features selected by feature selection methods and extracted into PCs by PCA can yield mixed results. For the DT and ANN, PCA increased the accuracy more than the original features from 95.50% and 96.31% to 96.64% and 96.59%. Similarly, feature selection outperformed the original features in the DT, ANN, and CNN with accuracy values of 95.92%, 96.59%, and 99.89%.

In addition, sensor redundancy in multilayer arrangement provides robust performance. The average score of all classifiers in all layers was better than that of a single layer for all feature arrangements, such as original, selected, extracted, and smoothed arrangements. The average prediction results for the combination of 3 layers is 99.72%, while those of layers 1, 2, and 3 are 97.15%, 96.29%, and 99.64%, respectively. Thus, the presence of sensors in all layers improved the discriminative ability in the classification process compared to the presence of only a set of sensors in a single layer.

The performance of our e-nose using a redundant array of sensors, with an accuracy average of 99.72%, has been in par and may exceed the performance of previous works in similar fields, as shown in Table 5. Some of these methods use e-noses, whereas others use near-infrared spectroscopy or colorimetric sensors coupled with machine learning algorithms. Thus, the proposed e-nose method exhibits improved classification accuracy.

Table 5. Previous studies on meat adulteration detection

Field	Method	Accuracy (%)	Ref
Adulterated lamb with duck	e-nose and near-infrared (NIR) spectroscopy using BPNN and SVM	98.59	[14]
Adulterated beef with pork	ensemble learning using KNN	98.33	[55]
Adulterated beef with pork	e-nose using SVM	98.1	[16]
Adulterated lamb with pork	Visible NIR using partial least squares discriminant analysis (PLSDA)	97.3	[56]
Adulterated beef with pork	Visible NIR using SVM, DT	97	[57]
Adulterated beef with pork	e-nose using SVM	95.71	[58]
Adulterated beef with pork	Colorimetric sensors using ELM & Fisher LDA	91.27	[15]

3.7. Discussion

The obtained data set of 8 sensors, 3 layers, and 15 classes shows a distinguishable pattern among classes from at least one of the sensors, which allows for accurate categorization. Feature selection and PCA help reduce the number of features used during classification. Feature selection can also identify the most important features, namely the MQ138, MQ 137, and MQ136. Among the preprocessing techniques, smoothing and feature selection provided better classification results than the use of the original dataset. Among the classifiers, the CNN yielded better accuracy than the other classifiers. Our hypothesis regarding redundant layers was supported by the best classification results for all layers compared to each layer (Table 4).

A previous study of e-nose to detect adulteration of lamb and duck meat using a combination of a BPNN and SVM, obtaining an accuracy of 98.6% [14], while the one to detect pork adulteration with beef using optimized SVM obtains an accuracy of 98.1% [16]. In terms of classification performance, this study achieved an average performance of all classifiers of 99.7% on all sensor layers. In addition, each layer obtained accuracy values of 97.15%, 96.29%, and 99.64%, respectively. On our dataset, the optimized SVM performed quite well, as it could reach an accuracy of 99.36%, but it still was close behind the optimized CNN, which yielded a prediction accuracy of 99.82%. The strength of the proposed approach lies in the use of a combination of layers, as there are more pools of sensors to choose from compared to a single layer. The use of an optimized 1D CNN for the time-series dataset demonstrated strong performance. The experimental setup of our approach still has limitations, as we must clean the chamber manually before measuring each sample. There are unexpected results that we encounter, such as the accuracy of layer 2, which lies between two other layers, being less than that of layer 1, which is placed in the furthest position.

In this study, redundant layers of a gas sensor were employed to detect the adulteration of beef with pork using an optimized CNN. Sensor redundancy reduces the risk of single sensor errors and improves the ability to detect beef adulteration. In addition, this study confirmed the feasibility of a 1D CNN for time-series datasets, especially for gas sensors. In future, the layer placement scheme should be experimentally rearranged so that all layers can contribute more optimally. The study can also be expanded using different types of adulterated objects or by designing a more portable system for use on a larger scale.

4. CONCLUSION

This study proposes a redundant gas sensor array for robust adulterated beef detection using a 1D CNN. The sensor chamber has 3 layers, and each layer contains 8 different gas sensors. The meat samples were categorized into 15 mixing classes of pork and beef ratios ranging from 0% to 100%. The dataset contains 5,400 samples and includes 360 samples per class. CNN was proposed as the primary classification method because of its ability to capture time-series patterns from sensor readings. The parameters of each classifier were optimized by cross-validation of the training data. Feature selection, feature extraction, and smoothing were performed to determine their effects on the classification results.

The test results demonstrate that the CNN yielded a prediction accuracy of 99.82%. This result is higher than that of other classifiers for data with selected, extracted, and smoothed features. The next best classifier was SVM with an accuracy of 99.36%, followed by KNN with an accuracy of 98.62%; ANN with an accuracy of 96.67%; and DT with an accuracy of 96.53%. In addition, smoothing can improve accuracy compared to the original feature. However, feature selection and PCA can only improve a few classifiers. Nevertheless, feature selection information can be obtained regarding the most influential sensor types, such as MQ138_3, MQ137_3, MQ137_2, MQ137_1, and MQ136_1. Similarly, a few PCs can represent almost all features. In addition, combining three layers provides better classification results than a single layer in terms of redundant sensor arrays. For a single-layer sensor configuration, the average CNN classification success rates were 97.15%, 96.29%, and 99.64% for layers 1, 2, and 3, respectively. In addition, for the combination of the three layers, the prediction results improved to 99.72%.

In future work, the placement of sensor layers should be further analyzed to optimize the contributions of all layers. The use of other objects can also expand the applicability of the proposed system. In addition, to increase the use of this halal meat detection system, it is crucial to design a portable system for the public.

ACKNOWLEDGEMENTS

This research received support from the Research Organization for Electronics and Informatics, National Research and Innovation Agency of the Republic of Indonesia.

FUNDING INFORMATION

This research received funding from the Research Organization for Electronics and Informatics, National Research and Innovation Agency of the Republic of Indonesia. This item is denoted as B-298/III.6/PR.03/1/2023 and is dated 20 January 2023 in Bandung.

AUTHOR CONTRIBUTIONS STATEMENT

This journal uses the Contributor Roles Taxonomy (CRediT) to recognize individual author contributions, reduce authorship disputes, and facilitate collaboration.

Name of Author	C	M	So	Va	Fo	I	R	D	O	E	Vi	Su	P	Fu
Ardani Cesario Zuhri	✓	✓	✓			✓	✓	✓	✓	✓			✓	✓
Agus Widodo		✓	✓	✓	✓				✓	✓	✓	✓		
Mario Ardhany	✓					✓		✓	✓	✓	✓			
Danny Mokhammad Gandana	✓			✓			✓			✓		✓	✓	✓
Galang Ilman Islami			✓			✓		✓	✓					
Galuh Prihantoro			✓		✓					✓	✓			

C : Conceptualization

M : Methodology

So : Software

Va : Validation

Fo : Formal analysis

I : Investigation

R : Resources

D : Data Curation

O : Writing - Original Draft

E : Writing - Review & Editing

Vi : Visualization

Su : Supervision

P : Project administration

Fu : Funding acquisition

CONFLICT OF INTEREST STATEMENT

Authors state no conflict of interest.

DATA AVAILABILITY

The data that support the findings of this study are available from the corresponding author, [initials, ACZ], upon reasonable request.

REFERENCES




- [1] B. M. Bohrer, "An investigation of the formulation and nutritional composition of modern meat analogue products," *Food Science and Human Wellness*, vol. 8, no. 4, pp. 320–329, 2019, doi: 10.1016/j.fshw.2019.11.006.
- [2] B. Kuswandi, A. A. Gani, and M. Ahmad, "Immuno strip test for detection of pork adulteration in cooked meatballs," *Food Bioscience*, vol. 19, pp. 1–6, 2017, doi: 10.1016/j.fbio.2017.05.001.
- [3] J. Ha *et al.*, "Identification of Pork Adulteration in Processed Meat Products Using the Developed Mitochondrial DNA-Based Primers," *Korean Journal for Food Science of Animal Resources*, vol. 37, no. 3, pp. 464–468, 2017, doi: 10.5851/kosfa.2017.37.3.464.
- [4] A. Szyłak, W. Kostrzewa, J. Bania, and A. Tabiś, "Do You Know What You Eat? Kebab Adulteration in Poland," *Foods*, vol. 12, no. 18, 2023, doi: 10.3390/foods12183380.
- [5] A. Mustapha, I. Ishak, N. N. M. Zaki, M. R. Ismail-Fitry, S. Arshad, and A. Q. Sazili, "Application of machine learning approach on halal meat authentication principle, challenges, and prospects: A review," *Heliyon*, vol. 10, no. 12, p. e32189, 2024, doi: 10.1016/j.heliyon.2024.e32189.
- [6] Q. Wang *et al.*, "Adulterant identification in mutton by electronic nose and gas chromatography-mass spectrometer," *Food Control*, vol. 98, pp. 431–438, 2019, doi: 10.1016/j.foodcont.2018.11.038.

- [7] E. M. Achata *et al.*, "Multivariate optimization of hyperspectral imaging for adulteration detection of ground beef: Towards the development of generic algorithms to predict adulterated ground beef and for digital sorting," *Food Control*, vol. 153, p. 109907, 2023, doi: 10.1016/j.foodcont.2023.109907.
- [8] C. Yang *et al.*, "Detection and characterization of meat adulteration in various types of meat products by using a high-efficiency multiplex polymerase chain reaction technique," *Frontiers in Nutrition*, vol. 9, 2022, doi: 10.3389/fnut.2022.979977.
- [9] A. Dashti *et al.*, "Assessment of meat authenticity using portable Fourier transform infrared spectroscopy combined with multivariate classification techniques," *Microchemical Journal*, 2022, doi: 10.1016/j.microc.2022.107735.
- [10] M. K. Woźniak *et al.*, "Development and validation of a GC–MS/MS method for the determination of 11 amphetamines and 34 synthetic cathinones in whole blood," *Forensic Toxicology*, vol. 38, pp. 42–58, 2020, doi: 10.1007/s11419-019-00485-y.
- [11] M. Ardhany *et al.*, "Early Detection of Motor Vehicle Exhaust Gas Using a Gas Sensor Array with Multiple Kernel Learning," *Evergreen*, vol. 11, no. 3, pp. 2678–2690, Sep. 2024, doi: 10.5109/7236907.
- [12] M. M. Bordbar, J. Tashkhourian, A. Tavassoli, E. Bahramali, and B. Hemmateenejad, "Ultrafast detection of infectious bacteria using optoelectronic nose based on metallic nanoparticles," *Sensors and Actuators B: Chemical*, vol. 319, p. 128262, 2020, doi: 10.1016/j.snb.2020.128262.
- [13] S. Grassi, S. Benedetti, M. Opizzio, E. Di Nardo, and S. Buratti, "Meat and fish freshness assessment by a portable and simplified electronic nose system (Mastersense)," *Sensors (Switzerland)*, vol. 19, no. 14, 2019, doi: 10.3390/s19143225.
- [14] W. Jia, Y. Qin, and C. Zhao, "Rapid detection of adulterated lamb meat using near infrared and electronic nose: A F1-score-MRE data fusion approach," *Food Chemical*, vol. 439, p. 138123, 2024, doi: 10.1016/j.foodchem.2023.138123.
- [15] F. Han, X. Huang, J. H. Aheto, D. Zhang, and F. Feng, "Detection of Beef Adulterated with Pork Using a Low-Cost Electronic Nose Based on Colorimetric Sensors," *Foods*, vol. 9, no. 2, 2020, doi: 10.3390/foods9020193.
- [16] R. Sarno, K. Triyana, S. I. Sabilla, D. R. Wijaya, D. Sunaryono, and C. Fatichah, "Detecting Pork Adulteration in Beef for Halal Authentication using an Optimized Electronic Nose System," *IEEE Access*, 2020, doi: 10.1109/ACCESS.2020.3043394.
- [17] A. Mirzaei, B. Hashemi, and K. Janghorban, "α-Fe₂O₃ based nanomaterials as gas sensors," *Journal of Materials Science: Materials in Electronics*, vol. 27, no. 4, pp. 3109–3144, 2016, doi: 10.1007/s10854-015-4200-z.
- [18] A. Fentaye, V. Zaccaria, and K. Kyprianidis, "Sensor Fault/Failure Correction and Missing Sensor Replacement for Enhanced Real-time Gas Turbine Diagnostics," *PHM Society European Conference*, vol. 7, no. 1, 2022, doi: 10.36001/phme.2022.v7i1.3315.
- [19] N. Trapani and L. Longo, "Fault Detection and Diagnosis Methods for Sensors Systems: a Scientific Literature Review," in *IFAC-PapersOnLine*, vol. 56, no. 2, 2023, doi: 10.1016/j.ifacol.2023.10.1749.
- [20] A.-M. Oncescu and A. Cicirello, "A Self-supervised Classification Algorithm for Sensor Fault Identification for Robust Structural Health Monitoring," in *European Workshop on Structural Health Monitoring*, 2023, vol. 253, pp. 564–574, doi: 10.1007/978-3-031-07254-3_57.
- [21] N. Cholis Basjaruddin and Y. Priyana, "Fault Tolerant Air Bubble Sensor using Triple Modular Redundancy Method," *TELKOMNIKA (Telecommunication Computing Electronics and Control)*, vol. 11, no. 1, pp. 71–78, 2013, doi: 10.12928/telkomnika.v11i1.884.
- [22] Y. Yin, F. Xu, and B. Pang, "Online intelligent fault diagnosis of redundant sensors in PWR based on artificial neural network," *Frontiers in Energy Research*, vol. 10, Sep. 2022, doi: 10.3389/fenrg.2022.1011362.
- [23] S. S. N. Chakravartula, R. Moschetti, G. Bedini, M. Nardella, and R. Massantini, "Use of convolutional neural network (CNN) combined with FT-NIR spectroscopy to predict food adulteration: A case study on coffee," *Food Control*, vol. 135, p. 108816, 2022, doi: 10.1016/j.foodcont.2022.108816.
- [24] F. Sultana, A. Sufian, and P. Dutta, "Advancements in Image Classification using Convolutional Neural Network," in *2018 Fourth International Conference on Research in Computational Intelligence and Communication Networks (ICRCICN)*, 2018, pp. 122–129, doi: 10.1109/ICRCICN.2018.8718718.
- [25] Z. Cahya, D. Cahya, T. Nugroho, A. Zuhri, and W. Agusta, "CNN Model with Parameter Optimisation for Fine-Grained Banana Ripening Stage Classification," in *Proceedings of the 2022 International Conference on Computer, Control, Informatics and Its Applications*, in IC3INA '22. New York, NY, USA: Association for Computing Machinery, 2023, pp. 90–94, doi: 10.1145/3575882.3575900.
- [26] J. Yim, J. Ju, H. Jung, and J. Kim, "Image Classification Using Convolutional Neural Networks with Multi-stage Feature," in *Robot Intelligence Technology and Applications 3*, Eds., Cham: Springer International Publishing, 2015, pp. 587–594, doi: 10.1007/978-3-319-16841-8_52.
- [27] B. K. O. C. Alwawi and A. F. Y. Althabhaee, "Towards more accurate and efficient human iris recognition model using deep learning technology," *TELKOMNIKA (Telecommunication Computing Electronics and Control)*, vol. 20, no. 4, pp. 817–824, Aug. 2022, doi: 10.12928/telkomnika.v20i4.23759.
- [28] M. Markova, "Convolutional neural networks for forex time series forecasting," *AIP Conference Proceedings*, vol. 2459, no. 1, p. 30024, 2022, doi: 10.1063/5.0083533.
- [29] A. Asesh and M. Dugar, "Time Series Prediction using Convolutional Neural Networks," in *2023 IEEE International Conference on Machine Learning and Applied Network Technologies (ICMLANT)*, 2023, pp. 1–6, doi: 10.1109/ICMLANT59547.2023.10372968.
- [30] J. Wang, X. Qiang, Z. Ren, H. Wang, Y. Wang, and S. Wang, "Time-Series Well Performance Prediction Based on Convolutional and Long Short-Term Memory Neural Network Model," *Energies (Basel)*, vol. 16, no. 1, 2023, doi: 10.3390/en16010499.
- [31] J. Hou, B. Adhikari, and J. Cheng, "DeepSF: Deep Convolutional Neural Network for Mapping Protein Sequences to Folds," in *Proceedings of the 2018 ACM International Conference on Bioinformatics, Computational Biology, and Health Informatics*, in BCB '18. New York, NY, USA: Association for Computing Machinery, 2018, p. 565, doi: 10.1145/3233547.3233716.
- [32] W. Huang *et al.*, "Identification of adulterated milk powder based on convolutional neural network and laser-induced breakdown spectroscopy," *Microchemical Journal*, vol. 176, p. 107190, 2022, doi: 10.1016/j.microc.2022.107190.
- [33] Misbah, M. Rivai, F. Kurniawan, D. Purwanto, S. Aulia, and Tasripan, "Electronic Nose using Convolutional Neural Network to Determine Adulterated Honeys," in *2022 International Conference on Computer Engineering, Network, and Intelligent Multimedia (CENIM)*, 2022, pp. 55–59, doi: 10.1109/CENIM56801.2022.10037552.
- [34] L. Fernandez, S. Marco, and A. Gutierrez-Galvez, "Robustness to sensor damage of a highly redundant gas sensor array," *Sensors and Actuators B: Chemical*, vol. 218, pp. 296–302, 2015, doi: 10.1016/j.snb.2015.04.096.
- [35] A. Kajmakovic, K. Diwold, K. Römer, J. Pestana, and N. Kajtazovic, "Degradation Detection in a Redundant Sensor Architecture," *Sensors*, vol. 22, no. 12, 2022, doi: 10.3390/s22124649.
- [36] S. Alelyani, J. Tang, and H. Liu, "Feature Selection for Clustering: A Review," in *Data Clustering*, Chapman and Hall/CRC, 2018, pp. 29–60, doi: 10.1201/9781315373515-2.

- [37] S. Šašić, T. Veriotti, T. Kotecki, and S. Austin, "Comparing the predictions by NIR spectroscopy based multivariate models for distillation fractions of crude oils by F-test," *Spectrochim Acta A Mol Biomol Spectrosc*, vol. 286, p. 122023, 2023, doi: 10.1016/j.saa.2022.122023.
- [38] P. Schober, C. Boer, and L. A. Schwarte, "Correlation Coefficients: Appropriate Use and Interpretation," *Anesthesia & Analgesia*, vol. 126, no. 5, 2018, doi: 10.1213/ANE.0000000000002864.
- [39] F. M. Canero, V. Rodriguez-Galiano, and D. Aragonés, "Machine Learning and Feature Selection for soil spectroscopy. An evaluation of Random Forest wrappers to predict soil organic matter, clay, and carbonates," *Heliyon*, vol. 10, no. 9, p. e30228, 2024, doi: 10.1016/j.heliyon.2024.e30228.
- [40] S. C. C. Sarkar and J. Srivastava, "Robust Feature Selection Technique Using Rank Aggregation," *Applied Artificial Intelligence*, vol. 28, no. 3, pp. 243–257, 2014, doi: 10.1080/08839514.2014.883903.
- [41] R. Zebari, A. M. Abdulazeez, D. Zeebaree, D. Zebari, and J. Saeed, "A Comprehensive Review of Dimensionality Reduction Techniques for Feature Selection and Feature Extraction," *Journal of Applied Science and Technology Trends*, vol. 1, pp. 56–70, May 2020, doi: 10.38094/jastt1224.
- [42] Q. Jiang, X. Yan, and B. Huang, "Performance-Driven Distributed PCA Process Monitoring Based on Fault-Relevant Variable Selection and Bayesian Inference," *IEEE Transactions on Industrial Electronics*, vol. 63, no. 1, pp. 377–386, 2016, doi: 10.1109/TIE.2015.2466557.
- [43] R. Bro and A. K. Smilde, "Principal component analysis," *Analytical Methods*, vol. 6, no. 9, pp. 2812–2831, 2014, doi: 10.1039/C3AY41907J.
- [44] N. Trendafilov and M. Gallo, "PCA and other dimensionality-reduction techniques," in *International Encyclopedia of Education (Fourth Edition)*, Fourth Edition., Eds., Oxford: Elsevier, 2023, pp. 590–599, doi: 10.1016/B978-0-12-818630-5.10014-4.
- [45] A. Widodo, I. Budi, and B. Widjaja, "Automatic lag selection in time series forecasting using multiple kernel learning," *International Journal of Machine Learning and Cybernetics*, vol. 7, no. 1, pp. 95–110, 2016, doi: 10.1007/s13042-015-0409-7.
- [46] S. Yoshida, K. Hatano, E. Takimoto, and M. Takeda, "Adaptive Online Prediction Using Weighted Windows," *IEICE TRANSACTIONS on Information and Systems*, vol. 94, no. 10, pp. 1917–1923, 2011, doi: 10.1587/transinf.E94.D.1917.
- [47] A. Casolaro, V. Capone, G. Iannuzzo, and F. Camastra, "Deep Learning for Time Series Forecasting: Advances and Open Problems," *Information*, vol. 14, no. 11, 2023, doi: 10.3390/info14110598.
- [48] J. M. Li, H. J. Wei, L. D. Wei, D. P. Zhou, and Y. Qiu, "Extraction of frictional vibration features with multifractal detrended fluctuation analysis and friction state recognition," *Symmetry (Basel)*, vol. 12, no. 2, 2020, doi: 10.3390/sym12020272.
- [49] P. Geladi and J. Linderholm, "2.03 - Principal Component Analysis," in *Comprehensive Chemometrics (Second Edition)*, Second Edi., Oxford: Elsevier, 2020, pp. 17–37, doi: 10.1016/B978-0-12-409547-2.14892-9.
- [50] S. Hasan, "An analysis using simulation to compare several moving average techniques for time series data," *Research Square*, pp. 1–6, 2023, doi: 10.21203/rs.3.rs-2540735/v1.
- [51] A. Ganjanesh, S. Gao, and H. Huang, "EffConv: Efficient Learning of Kernel Sizes for Convolution Layers of CNNs," *Proceedings of the AAAI Conference on Artificial Intelligence*, vol. 37, no. 6, pp. 7604–7612, 2023, doi: 10.1609/aaai.v37i6.25923.
- [52] J. Nagi, A. Giusti, F. Nagi, L. M. Gambardella, and G. A. Di Caro, "Online feature extraction for the incremental learning of gestures in human-swarm interaction," in *2014 IEEE International Conference on Robotics and Automation (ICRA)*, 2014, pp. 3331–3338, doi: 10.1109/ICRA.2014.6907338.
- [53] N. Srivastava, G. Hinton, A. Krizhevsky, I. Sutskever, and R. Salakhutdinov, "Dropout: A Simple Way to Prevent Neural Networks from Overfitting," *Journal of Machine Learning Research*, vol. 15, no. 56, pp. 1929–1958, 2014.
- [54] S. Park and N. Kwak, "Analysis on the Dropout Effect in Convolutional Neural Networks," in *Computer Vision—ACCV 2016: 13th Asian Conference on Computer Vision, Taipei, Taiwan, November 20–24, 2016, Revised Selected Papers, Part II 13*, 2017, pp. 189–204, doi: 10.1007/978-3-319-54184-6_12.
- [55] M. Malikah, R. Sarno, and S. I. Sabilla, "Ensemble Learning for Optimizing Classification of Pork Adulteration in Beef Based on Electronic Nose Dataset," *International Journal of Intelligent Engineering and Systems*, vol. 14, no. 4, pp. 44–55, Aug. 2021, doi: 10.22266/ijies2021.0831.05.
- [56] X. Zuo, Y. Li, X. Chen, L. Chen, and C. Liu, "Rapid Detection of Adulteration in Minced Lamb Meat Using Vis-NIR Reflectance Spectroscopy," *Processes*, vol. 12, no. 10, 2024, doi: 10.3390/pr12102307.
- [57] A. Rady and A. Adedeji, "Assessing different processed meats for adulterants using visible-near-infrared spectroscopy," *Meat Science*, vol. 136, pp. 59–67, 2018, doi: 10.1016/j.meatsci.2017.10.014.
- [58] S. Wakhid, R. Sarno, and S. I. Sabilla, "The effect of gas concentration on detection and classification of beef and pork mixtures using E-nose," *Computers and Electronics in Agriculture*, vol. 195, p. 106838, 2022, doi: 10.1016/j.compag.2022.106838.

BIOGRAPHIES OF AUTHORS






Ardani Cesario Zuhri    holds a Bachelor of Engineering (B.Eng.) in Engineering Physics from Bandung Institute Technology. He is currently active in research and development for Indonesian government institutions, National Research and Innovation Agency. He is also a member of one of the research groups at the Research Center for Process and Manufacturing Industry Technology, which focuses on machine tools and production equipment. His most recent research interests include several recent research trends, such as machine learning and the internet of things. He can be contacted at email: arda004@brin.go.id.






Agus Widodo    holds a Bachelor of Science (B.Sc.) in Computer Science from Louisiana State University, USA, a joint Master Degree in Computer Science from ITS-Surabaya, Indonesia and Newcastle University, UK, and a Doctoral Degree in Computer Science from the University of Indonesia, Depok, Indonesia. He has been working as an engineer at the National Agency for Research and Innovation since 2022 and previously at the Agency for the Assessment and Application of Technology since 1995. His research areas of interest include machine learning, artificial intelligence, and technology forecasting. He can be contacted at email: agus.widodo@brin.go.id.






Mario Ardhan    holds a Bachelor of Engineering (S.T) in Engineering Physics from the Sepuluh Nopember Institute of Technology, Surabaya, Indonesia, in 2017. He has worked as an engineer for The Agency for the Assessment and Application of Technology (BPPT) Indonesia since 2020 and as a researcher for the National Research and Innovation Agency since 2022. His research areas of interest include artificial intelligence, machine learning, instrumentation, and machining. He can be contacted at email: mari026@brin.go.id.



Danny Mokhammad Gandana    holds Ph.D. in Dynamics and Control, Department of Aeronautical and Mechanical Engineering at Salford University, Salford, Manchester, United Kingdom. He is a principal engineer at the National Research and Innovation Agency, Indonesia, and a member of the Institute of Electrical and Electronics Engineers (IEEE). His research areas of interest include control system engineering, system dynamics artificial intelligent, mechatronics, and smart sensor. He can be contacted at email: dann001@brin.go.id.



Galang Ilman Islami    holds a Bachelor of Applied Science (B.A.Sc.) in Mechatronics Engineering. He is currently an engineer and research assistant at the National Research and Innovation Agency, Indonesia and a member of the research group of Machine Tools and Production. His research areas of interest include mechatronics, control system, and embedded system. He can be contacted at email: gala001@brin.go.id.



Galuh Prihantoro    received his Bachelor of Engineering in Informatics Engineering from the Islamic University of Indonesia and Master of Engineering in Electrical Engineering from University of Indonesia. He has worked as an engineer for The Agency for the Assessment and Application of Technology (BPPT) Indonesia since 2010 and has been working as a researcher for the National Research and Innovation Agency since 2022. His research areas of interest include image processing, artificial intelligent, control and application programming, and industrial automation. He can be contacted at email: galu005@brin.go.id.